九州工業大学学術機関リポジトリ

Kyutacar

Kyushu Institute of Technology Academic Repository

Design of Practical Superconducting DC Power Cable With REBCO Coated Conductors

Design of Practical Superconducting DC Power Cable with REBCO Coated Conductors

Vladimir S. Vyatkin, Masaru Kiuchi, Edmund S. Otabe and Teruo Matsushita

Abstract— The authors proposed an innovative superconducting DC power cable using the longitudinal magnetic field effect, i.e., a significant enhancement of the critical current density of a superconductor in a parallel magnetic field. It was expected that a cable with a high current-carrying capacity could be realized with $REBa_2Cu_3O_{7-\delta}$(REBCO) coated conductors. However, the critical current density in most commercial coated conductors does not increase but slightly decreases with increasing parallel magnetic field. Nevertheless, the critical current density in the parallel magnetic field is remarkably higher than that in a normal in-plane magnetic field, and it is possible to construct a DC cable with a higher current-carrying capacity using this characteristic in comparison with conventional superconducting cables. In this paper, we propose a new design of DC power cable suitable for present commercial coated conductors. The optimal condition of the cable is discussed.

Index Terms— High-temperature superconductors, superconducting DC cable, critical current density, longitudinal magnetic field effect.

I. INTRODUCTION

Superconducting power cables have been energetically developed based on the development of long high-temperature superconducting tapes with high critical currents. One of the potential applications of superconducting power cables is DC transmission of electric power generated by renewable sources such as sunshine and wind power. The DC power transmission is suitable for superconductivity that causes no energy dissipation in a steady condition. In addition, a simpler structure is also a merit of DC power cables than in AC power cables.

The authors proposed a new superconducting DC cable with high current-carrying capacity. It was reported that the critical current density was dramatically enhanced for a metallic superconductor in a parallel magnetic field in comparison with that in a normal magnetic field [1-6]. It was empirically known that a force-free structure for flux lines, i.e., a structure in which the current flowed parallel to flux lines, was established in this field configuration [7-9]. An employment of artificial force-free structure was predicted to significantly enhance the current-carrying capacity of the cable [10]. The essential point was to use the current flowing back on the outer shield conductor for applying an axial magnetic field to the inner conductor and the inner conductor was designed to be in the force-free structure under this axial magnetic field produced by the return current. As a result, the current-carrying capacity could be significantly enhanced in comparison with conventional superconducting DC cables [10]. Especially the enhancement factor increased with increasing current-carrying capacity because of stronger axial magnetic field.

However, the serious problem in present commercial coated conductors is that the critical current does not increase with increasing parallel magnetic field as in metallic superconductors [11]. Some high-quality superconducting thin films with the superconducting layer thickness below 0.5 μm showed a remarkable enhancement of the critical current density [12]. However, the structure of the superconducting layer is generally deteriorated with increasing layer thickness [13]. Especially it was found that *a*-axis grains and tilted *c*-axis grains tend to start to grow at a distance of about 0.5 μm from the substrate [14]. Thus, it is expected that the grain boundaries of these grains with the superconducting matrix meander the current, resulting in a decrease in the critical current density because of deviation from the force-free state. The degradation of the critical current density with increasing superconducting layer thickness [15-20] is consistent with the growth of such grains. Hopefully this situation can be overcome in the future by improving the fabrication process of coated conductors.

For this reason present commercial coated conductors are not useful to the force-free power cable. The same thing can be said to Bi-based superconductors. Then, the question is an investigation of a cable structure that can enhance the current-carrying capacity even for present common coated conductors and Bi-based superconductors.

II. PRELIMINARY INVESTIGATION

A better critical current property was obtained for a coated conductor fabricated by the Pulsed Laser Deposition (PLD) method on the Ion-Beam Assisted Deposition (IBAD) substrate among various coated conductors. This was probably caused by a better crystallinity of the superconducting layer for a YBCO coated conductor fabricated by this combination. The magnetic field dependence of the critical current density of this coated
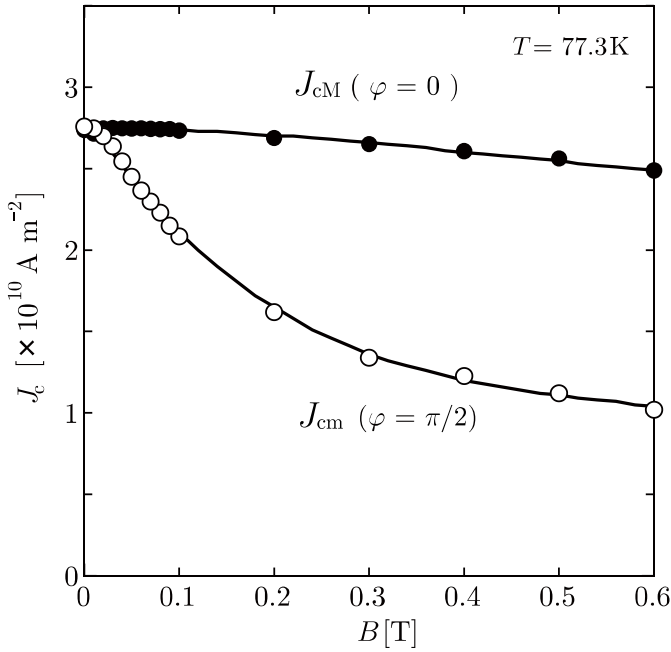
Fig. 1. Dependences of critical current density of a commercial coated conductor made by Fujikura Ltd. on parallel (solid symbols) and normal in-plane (open symbols) magnetic fields at 77.3 K. The solid lines show analytic approximations of Eq. (1) with expansion coefficients in Table I.

TABLE I
FITTING PARAMETERS FOR J_{cm} AND J_{cM}.

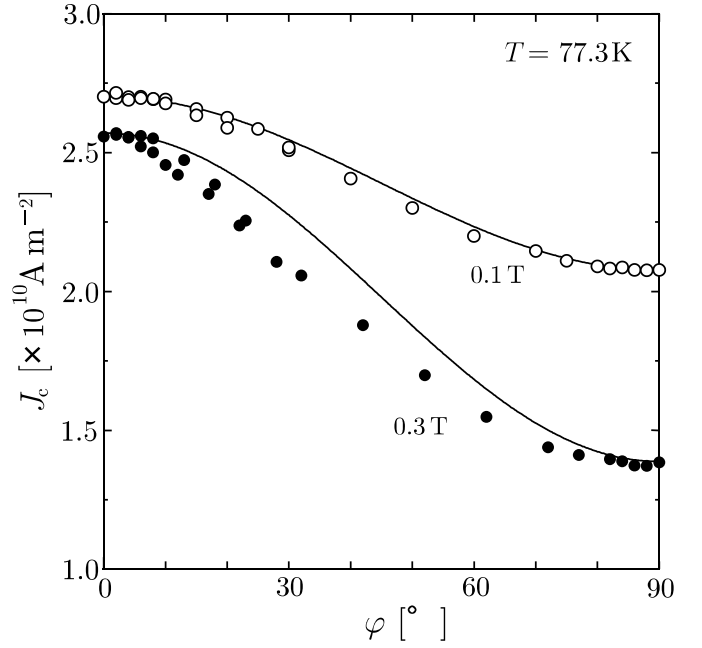| j	$K_{mj}[\times 10^{10} \mathrm{Am^{-2}/T^{j}}]$	$K_{Mj}[\times 10^{10} \mathrm{Am^{-2}/T^{j}}]$
0	2.738	2.738
1	-0.1780	0.4024
2	-168.3	-5.696
3	1623	26.00
4	-7618	-149.5
5	20682	678.3
6	-33854	-1716
7	32885	2308
8	-17433	-1560
9	3880	417.5

Fig. 2. In-plane field angle (φ) dependence of critical current density of a commercial coated conductor shown in Fig. 1 at 77.3 K. The solid lines show the characteristics assumed in Eq. (2).

conductor is shown in Fig. 1. It is found that the critical current density in a parallel magnetic field (J_{cM}) is almost constant or slightly decreases with increasing magnetic field. This is fairly higher than that in a normal in-plane magnetic field (J_{cm}), and this superior property can be used for a new power cable. The important thing is that, when the force-free structure is introduced to the cable, the outer layers in the inner conductor must be strongly twisted and the ratio of the transport current to the flowing current decreases significantly. That is, the ratio of the circulating current increases. When the outermost layer is twisted with the winding angle of $\pi/3$ for example, the ratio of the transport current in this layer decreases to half. Hence, if the critical current density does not increase more than twice, the employment of the force-free structure is not optimal, although it contributes to an enhancement of the currents in the inner layers through strengthening the axial field. It is considered that there is an optimal angle for twisting the layer, where the critical current density is relatively high and the transport efficiency is not appreciably decreased.

The authors proposed a new structure of superconducting DC cable based on this idea to attain a higher current-carrying capacity even for present commercial coated conductors [11, 21, 22]. In this paper this new structure is investigated in more detail to find out the optimal structure for each coated conductor. For the investigation of designing the optimal configuration, the field-angle dependence of the critical current density is important. The measurement of the dependence of the critical current density on the angle φ of the in-plane magnetic field was conducted. Figure 2 shows the results for the specimen shown in Fig. 1.

III. ANALYSIS

The current-carrying capacity of a superconducting DC power cable is investigated to discuss the optimal structure of the cable. The numerical analysis is based on the experimental results of Figs. 1 and 2. Analytical expressions of these results are necessary, therefore, for calculating the current-carrying capacity of the cable. For this purpose, the magnetic field dependence of the critical current densities in Fig. 1 are approximated as

$$J_{cm}(B) = \sum_{j=0}^{9} K_{mj} B^{j},$$

$$J_{cM}(B) = \sum_{j=0}^{9} K_{Mj} B^{j}, \tag{1}$$

where K_{mj}'s and K_{Mj}'s are expansion coefficients (see Table I). The solid lines in Fig. 1 show the above formulae. The in-plane field angle dependence of the critical current density is approximated as

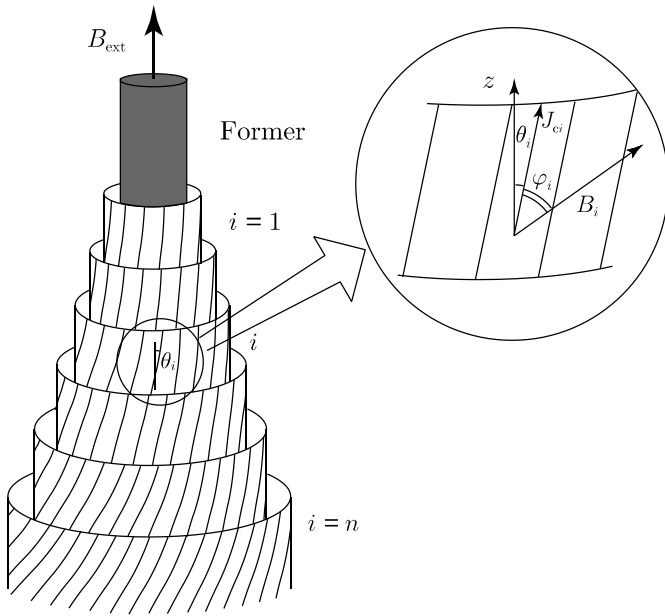$$J_{c}(\varphi) = \frac{1}{2}(J_{cM} + J_{cm}) + \frac{1}{2}(J_{cM} - J_{cm})\cos 2\varphi. \tag{2}$$

Fig. 3. Schematic illustration of winding structure of coated conductors in inner conductor. The angle θ_i for the current is measured from the cable axis, and φ_i is the angle between the current and magnetic field. The axial magnetic field produced by the outside shield conductor is B_{ext}.

The solid lines in Fig. 2 show this approximation.

The structure of the cable is defined. We treat the case where the inner conductor is composed of n layers of coated conductors aligned parallel on a cylindrical plane with the same angle θ_i in the i-th layer ($i = 1, 2, \cdots, n$). The radius of the i-th layer is denoted as

$$R_i = R_0 + id, \tag{3}$$

where R_0 is the radius of the inner former on which the coated conductors are wound and d is the sum of the thickness of the coated conductor and that of the isolation tape. For simplicity, it is assumed that there is no gap between adjacent coated conductors in the same layer (although small gaps will appear between adjacent conductors in a practical cable, it is expected that this does not appreciably affects the predicted current-carrying capacity). The angle of each layer is assumed to increase linearly for simplicity from the innermost layer angle, θ_1, to the outermost layer angle, θ_n. If the twisting angle of the outermost layer in a continuum model for an infinite n is denoted by θ_m, the i-th layer covers the field angle region between $(i-1)\theta_m/n$ and $i\theta_m/n$. Hence, we change the distribution of the twisting angle from that in Ref. 21 and determine in average as

$$\theta_i = \frac{(i - 1/2)}{n} \theta_m. \tag{4}$$

Then, the innermost layer is not parallel to the cable axis, and this is beneficial for winding the cable. We selected the linear angle distribution because the current-carrying capacity is deteriorated when the angle distribution changes from the linear one. The structure of the conductor is schematically illustrated in Fig. 3, where B_{ext} is the axial magnetic field produced by the current flowing in the outer shield conductor. The engineering critical current density is given by $J_e = \beta J_c$, where β is the fraction of the superconductor in the winding area. If the thickness of the superconducting layer is t, we have

$\beta = t/d$. The current flowing in the i-th layer is

$$I_i = 2\pi R_i J_{ei} d. \tag{5}$$

The magnetic field on each layer is formally described, and the magnetic field and critical current density must be solved self-consistently. The analysis method is described in Ref. 21. For convenience it is given in Appendix.

IV. RESULTS AND DISCUSSION

The current-carrying capacity of the new cable with 6 - 12 layers are calculated under various conditions of the external axial magnetic field, B_{ext}, produced by the return current. It is assumed that $R_0 = 20$ mm, $d = 200$ μm and $t = 2.00$ μm.

Figure 4 shows the current-carrying capacity of a cable with 8-layers ($n = 8$) as a function of θ_m in various values of B_{ext}. Windings of superconducting tapes in usual superconducting DC cables are essentially the same as those in AC cables. In these cables, the superconducting layers are twisted with positive and negative angles, so that the axial magnetic field is eliminated to reduce additional AC losses. Hence, the structure is different from that shown in Fig. 3. Such cables are assumed as conventional cables. In this case, the self-field is directed almost normal to the axis of the cable. Hence, for the calculation of the current-carrying capacity of conventional cables, we can assume $\varphi = \pi/2$, and it corresponds to the point at $\theta_m = 0$ for $B_{\text{ext}} = 0$ in Fig. 4. It is found that the current-carrying capacity can be enhanced from that in the conventional cable over a wide region of θ_m and B_{ext}. The current-carrying capacity increases with increasing the angle θ_m and takes a peak and then, tends to decrease. The first increase comes from the effect of the axial self-field due to the current that increases the critical current density, and the accompanied decrease is caused by a reduction in the transport
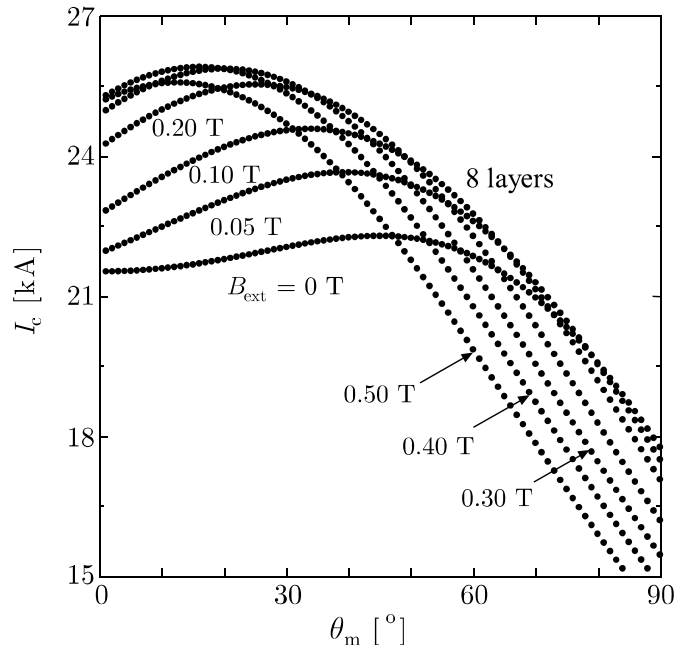

Fig. 4. Current-carrying capacity vs. θ_m in various values of external longitudinal magnetic field B_{ext} for $n = 8$.
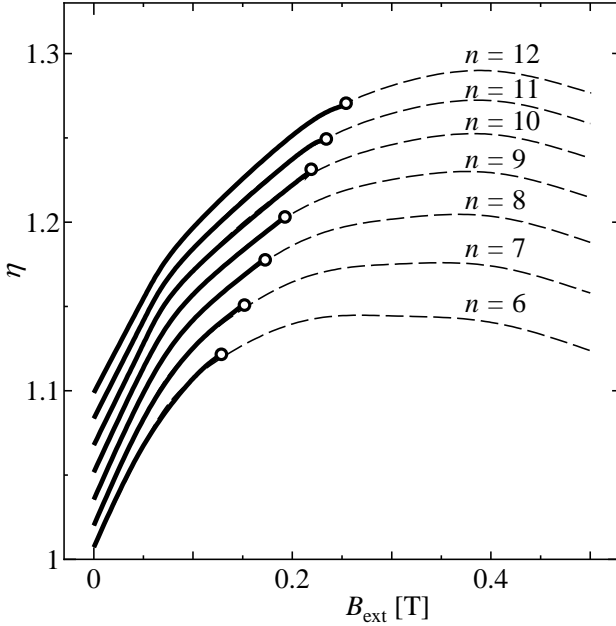
Fig. 5. Transport efficiency vs. external axial magnetic field. The solid lines show attainable regions and the open symbols show the optimal conditions for each layer number. The dashed curves show unrealized efficiencies limited by the current in the shield conductor.

efficiency. It is found that the value of θ_m at the peak capacity is much lower than that for the force-free cable, $\theta_m \cong 53°$ [10]. It clearly shows that there is no merit to realize the ideal force-free configuration and a choice of a slight increase in the critical current density by lowering the Lorentz force is better. The current-carrying capacity increases with B_{ext} so long as B_{ext} is small. This comes from the enhancement of the critical current density by reducing the magnetic field angle. When B_{ext} becomes large, the current-carrying capacity decreases with increasing B_{ext}. This is because the axial magnetic field dependence of the critical current density is weak.

It should be noted here that B_{ext} is produced by the current flowing back in the shield conductor and hence, it is a function of I_c. That is, there is an achievable limit of the B_{ext}-value. Here, the maximum value of $B_{ext}(B_{extm})$ is determined. We assume that the mean radius and twisting angle of the shield conductor are R_s and θ_s, respectively. If the helical current flowing in the shield conductor is I_c', the transport current must be the same: $I_c' \cos \theta_s = I_c$. Then, the external longitudinal magnetic field is formally given by

$$B_{ext} = \frac{\mu_0 I_c' \sin \theta_s}{2\pi R_s} = \frac{\mu_0 I_c}{2\pi R_s} \tan \theta_s. \quad (6)$$

This must be solved self-consistently to obtain the achievable values of B_{ext} and I_c. For this purpose the iteration method is used again. Here, we assume as $R_s = 25$ mm and $\theta_s = 40°$.
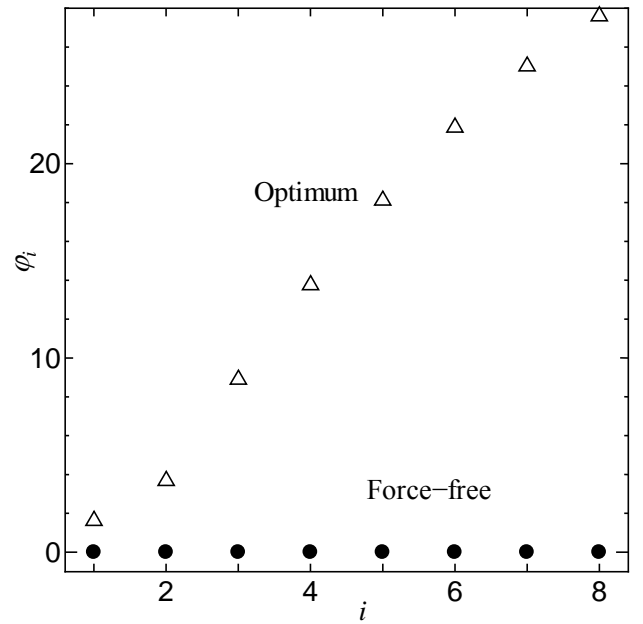
The transport efficiency of the cable is defined by the ratio of the maximum current-carrying capacity, I_{cm}, of the new cable for various θ_m values to that in the conventional superconducting DC cable, I_0;

$$\eta = \frac{I_{cm}}{I_0}. \quad (7)$$

The dependence of the transport efficiency on B_{ext} is shown in
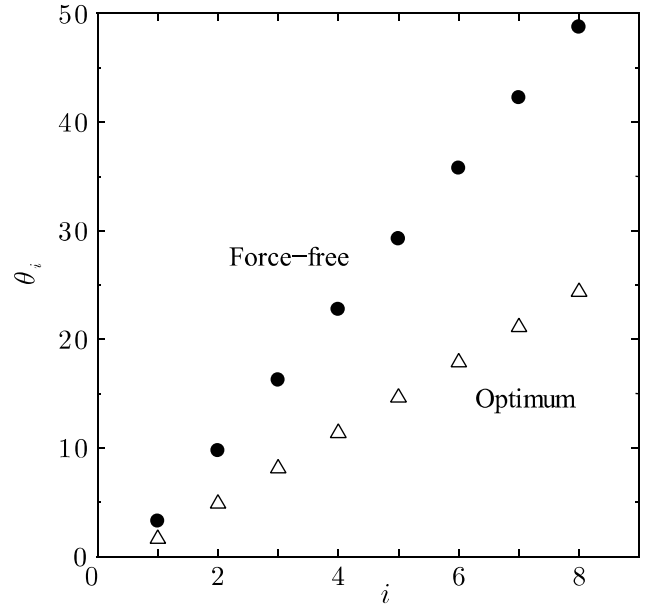
(a)

(b)

Fig. 6. (a) Distributions of twisting angle θ_i and (b) angle φ_i of magnetic field from the superconductor axis for the present optimal cable and the ideal force-free cable for $n = 8$.

Fig. 5. The dashed curves show virtual efficiencies for which B_{ext} cannot be realized by the current flowing back in the shield conductor. The achievable regions and maximum transport efficiencies are shown by solid lines and open symbols, respectively. The corresponding values of θ_m are shown in Table II. The transport efficiency increases monotonically with increasing layer number n and/or B_{ext}. Hence, if we could

TABLE II
OPTIMUM TWISTING ANGLE FOR DIFFERENT LAYER NUMBERS N IN CASE OF $R_s = 25$ MM AND $\theta_s = 40°$.

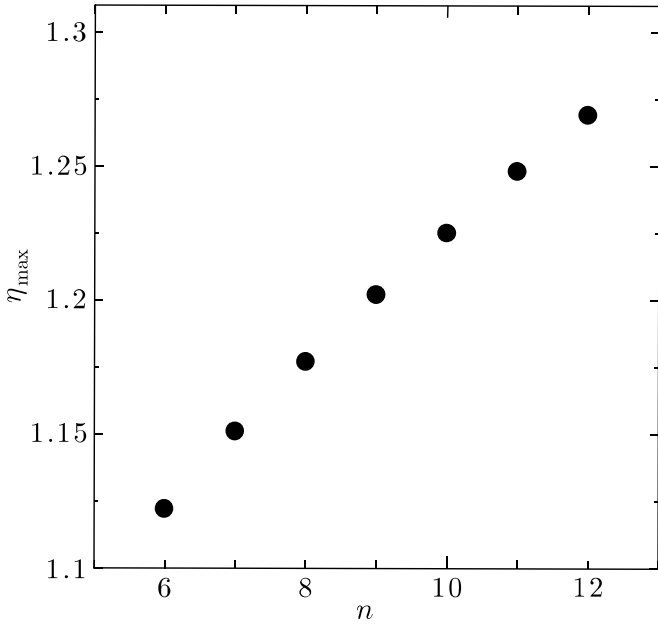| n	6	7	8	9	10	11	12
$\theta_m[°]$	25	26	27	28	29	30	30

Fig. 7. Maximum transport efficiency of cable vs. layer number.

TABLE III
CURRENT-CARRYING CAPACITY OF CONVENTIONAL CABLE (I_0), ACHIEVABLE
EXTERNAL AXIAL MAGNETIC FIELD (B_{EXTM}), MAXIMUM CURRENT-CARRYING
CAPACITY OF NEW CABLE (I_{EXTM}) AND MAXIMUM TRANSPORT EFFICIENCY (η_{MAX})
FOR EACH LAYER NUMBER (N) IN CASE OF $R_s = 25$ MM AND $\theta_s = 40°$.

n	I_0[kA]	B_{extm}[T]	I_{cmax}[kA]	η_{max}
6	17.18	0.1294	19.27	1.122
7	19.39	0.1498	22.31	1.151
8	21.52	0.1701	25.34	1.177
9	23.59	0.1903	28.35	1.202
10	25.60	0.2106	31.37	1.225
11	2756	0.2309	34.39	1.248
12	29.48	0.2511	37.41	1.269

TABLE IV
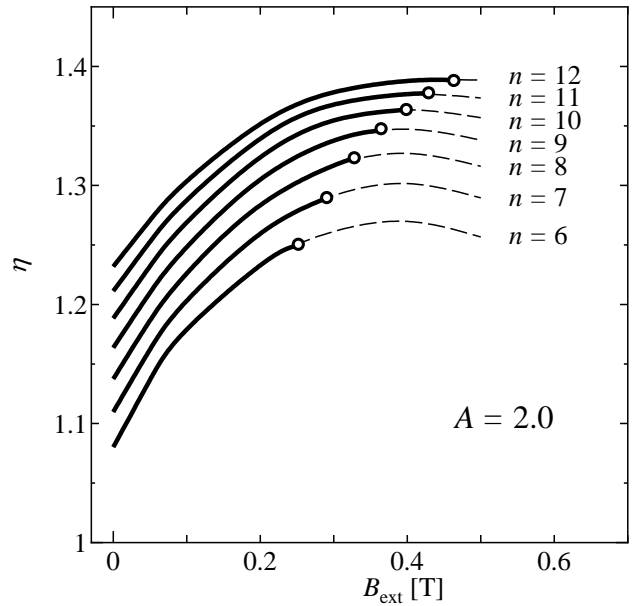MAXIMUM TRANSPORT EFFICIENCY FOR DIFFERENT COMBINATIONS OF R_s
AND θ_s.

n	$R_s = 25$ mm		$R_s = 30$ mm
	$\theta_s = 30°$	$\theta_s = 35°$	$\theta_s = 40°$
6	1.099	1.111	1.111
7	1.126	1.139	1.139
8	1.151	1.165	1.165
9	1.175	1.189	1.189
10	1.197	1.212	1.212
11	1.218	1.234	1.234
12	1.238	1.254	1.254

(a)

(b)

Fig. 8. Transport efficiency vs. external axial magnetic field when the critical current density is simply improved by factors (a) A=1.5 and (b) A=2.0. The dashed curves show unrealized efficiencies.

improve the critical current density of the coated conductor, the achievable transport efficiency would be increased more through the increase in B_{extm}. This will be discussed later.

Here we discuss the difference of the present cable and the ideal force-free cable. In the case of $n = 8$, the maximum transport efficiency of the present cable is 1.18, while that of the force-free cable is 2.13 [10]. This large difference comes

from the difference in the critical current density in parallel magnetic field. As a result, the force free state cannot be selected, since transport efficiency decreases appreciably. The distributions of twisting angle are compared in Fig. 6(a). The distribution is strictly determined so that the magnetic field is parallel to the superconducting tape: It can be seen that the superconductors are more tightly twisted in the force-free cable: $\theta_m = \mu_0 J_{\mathrm{cM}} n d / B$ with B being a magnetic field which is constant throughout the cable [10]. This is possible, since there is a room of twisting. That is, although the twisting lowers the rate of the transport current, the enhancement of the critical current density is sufficiently high to cover this factor. As a result, the force-free state, in which the magnetic field and the
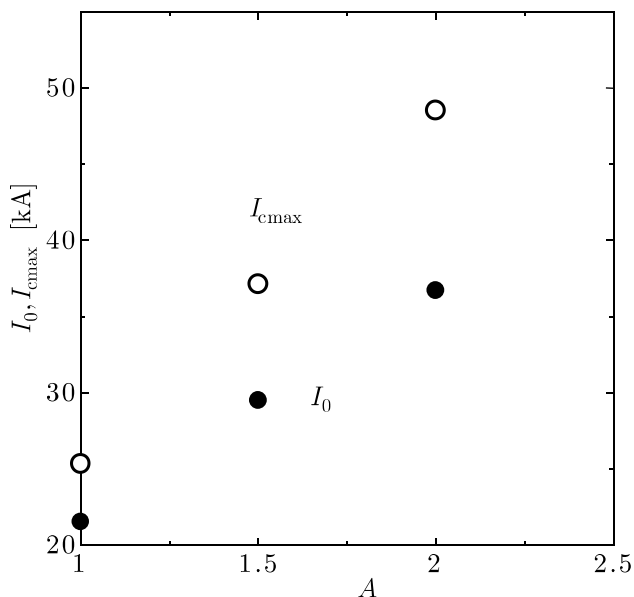
Fig. 9. Current-carrying capacity vs. improvement factor A of critical current density for proposed and conventional cables.

current are parallel to each other, can be realized as shown in Fig. 6(b). If the dependence of the critical current density on the parallel magnetic field is improved, the optimal distribution of the present cable will get closer to that of the force-free cable.

The relationship between η_{max} and layer number n is shown in Fig. 7. It can be seen that η_{max} monotonically increases with n. The obtained results for n from 6 to 12 are summarized in Table III.

The obtained results in Fig. 5 indicates that, if we could improve the critical current density of coated conductor, the achieved transport efficiency would be increased more through the increase in B_{extm}. In fact, if the critical current densities in Eq. (1) are simply improved by factor A=1.5 or 2.0, the transport efficiency is predicted to be improved as shown in Fig. 8(a) or (b), respectively. This seems to be a practical method to improve the efficiency, since it may take many years to essentially improve the longitudinal field effect of coated conductors. Figure 9 compares the current-carrying capacity between the present and conventional cables as a function of the improvement factor of the critical current density. It is found that the current-carrying capacity of the present cable increases almost linearly with increasing the critical current density, while that in the conventional cable tends to be saturated because of the enhanced self-field. This also shows that the proposed cable is suitable for transportation of large currents.

The calculated results for different values of R_s and θ_s are listed in Table IV. When R_s is increased or θ_s is decreased, η_{max} decreases because of the decrease in B_{ext}. Even for $R_s = 25$ mm and $\theta_s = 40°$, however, the value of η_{max} is about 1.27 for $n = 12$, and the current-carrying capacity can be appreciably increased from the conventional cables.

Thus, the proposed design of superconducting DC cable is effective for improving the current-carrying capacity even for present coated conductors that do not show a remarkable enhancement of the critical current density in a parallel

magnetic field. Recently it was shown [21] that the current-carrying capacity of a one layer cable made with Bi-2223 tapes had a peak value under the condition where the magnetic field was parallel to the tapes, and a similar result was obtained for a one layer cable made with REBCO coated conductors [24]. This shows that the proposed cable structure is promising. The key point of this structure is to enhance the ratio of the transport current and to utilize a merit of reducing the Lorentz force. The optimal design is different depending on the critical current density properties of coated conductors, and if the critical current density is improved, an achievement of much higher current-carrying capacity can be expected. The important point is that this structure can be applied to cables fabricated with Bi-based superconductors.

One practical problem in the proposed structure is that the twisting angle in the optimized conductor is too small for i=1 and 2 in Fig. 6(a). Such almost straight winding makes it difficult to bend the cable. The low winding angles might be increased to around 10°. Then, the current-carrying capacity of the cable will be slightly reduced from the present estimation by this change.

However, we have to bear in mind that the force-free cable is of the best efficiency. Hence, efforts should be made to improve the critical current density of coated conductors in a longitudinal magnetic field to realize the force-free cable in the future. For this purpose it is important at first to improve the weak link behavior by eliminating a-axis and tilted c-axis grains in the superconducting layer in coated conductors. The next step is to improve directly the critical current properties. The mechanism that determines the critical current density in the superconductor in the longitudinal magnetic field is not the flux cutting [25-28] but flux pinning [3, 29-31]. That is, the balance between the force-free torque to reduce the torsional shear of flux lines and the pinning torque determines the critical current density [32, 33], in an analogous manner to the balance between the Lorentz force and the pinning force in transverse magnetic field. The pinning centers effective for enhancement of the critical current density in this field configuration are those that prevent flux lines from rotating in the a-b plane to reduce the torsional shear. Introduction of such pinning centers will contribute to a further improvement of the critical current density.

V. Summary

A new design is proposed for superconducting DC power cable with present commercial coated conductors. It is found that the current-carrying capacity can be significantly enhanced from conventional cables, although the critical current density decreases slightly with increasing parallel magnetic field. Therefore, this theoretical approach provides a practical design suitable for each coated conductor with different critical current density. It should be noted that this design can also be used for Bi-based superconductors. It is expected to practically examine a feasibility of this design of DC cable. At the same time,

efforts should be made to improve the critical current density of coated conductors in a parallel magnetic field to realize the force-free cable in the future, because the current-carrying capacity of the force-free cable is much higher than that in cables with the present structure.

APPENDIX

The critical state is assumed for every layer to estimate the current-carrying capacity. The current flowing in the i-th layer produces an axial magnetic field

$$B'_{i\parallel} = \frac{\mu_0 I_i \cos\theta_i}{L_i} = \frac{\mu_0 I_i \sin\theta_i}{2\pi R_i}, \tag{8}$$

in the inner region ($R < R_i$), where $L_i = 2\pi R_i \cot\theta_i$ is the winding pitch of the i-th layer. The azimuthal magnetic field produced outside the i-th layer ($R < R_i$) is

$$B'_{i\perp} = \frac{\mu_0 I_i \cos\theta_i}{2\pi R}. \tag{9}$$

Hence, if the external axial magnetic field produced by the return current flowing in the shield conductor is B_{ext}, the axial and azimuthal magnetic fields on the i-th layer are

$$B_{i\parallel} = \sum_{k=i+1}^{n} \frac{\mu_0 I_k \sin\theta_k}{2\pi R_k} + B_{\text{ext}} \tag{10}$$

and

$$B_{i\perp} = \sum_{k=1}^{i-1} \frac{\mu_0 I_k \cos\theta_k}{2\pi R}, \tag{11}$$

respectively. Then, the strength of the magnetic field on the i-th layer is

$$B_i = \left(B_{i\parallel}^2 + B_{i\perp}^2\right)^{1/2}, \tag{12}$$

and its angle from the direction of the tape is

$$\varphi_i = \theta_i - \tan^{-1}\frac{B_{i\perp}}{B_{i\parallel}}. \tag{13}$$

The transport current of the i-th layer is $I_i \cos\theta_i$ and the current-carrying capacity of the cable is

$$I_c = \sum_{i=1}^{n} I_i \cos\theta_i. \tag{14}$$

The critical current density of the i-th layer is given by

$$\begin{aligned} J_c(\varphi_i) &= \frac{1}{2}\big(J_{cM}(B_i) + J_{cm}(B_i)\big) \\ &\quad + \frac{1}{2}\big(J_{cM}(B_i) \\ &\quad - J_{cm}(B_i)\big)\cos 2\varphi_i \\ &= J_{ci}. \end{aligned} \tag{15}$$

There are n sets of the above equations. These set of equations can be numerically calculated using the iteration method:

$$J_{ci} = f(J_{c1}, J_{c2}, \cdots, J_{cn}). \tag{16}$$

In the initial condition we assume that all layers have the same critical current densities $J_{c1}^{(0)} = \cdots = J_{c1}^{(0)} = J_{cM}(B=0)$, and the calculation of the next step is done with obtained critical current densities in each layer. The calculation is iterated until an unchanged set of solutions are obtained. In Ref. 21 it was shown that the iteration method can reproduce the results of analytic solution for the ideal force-free case.

On the other hand, the current-carrying capacity I_0 in usual superconducting cable in the azimuthal magnetic field is simply obtained by putting $B_{\text{ext}} = 0$ and $\varphi = \pi/2$ ($\theta_m = 0$).

REFERENCES

[1] S. T. Sekula, R. W. Boom and C. J. Bergeron, "Longitudinal critical currents in cold‐drawn superconducting alloys," *Appl. Phys. Lett.*, vol. 2, p. 102, 1963.

[2] G. W. Cullen, G. D. Cody and J. P. McEvoy, Jr., "Field and Angular Dependence of Critical Currents in Nb₃Sn," *Phys. Rev.*, vol. 132, p. 577, 1963.

[3] G. W. Cullen and R. L. Novak, "Effect of fast‐neutron‐induced defects on the current carrying behavior of superconducting Nb₃Sn," *Appl. Phys. Lett.*,vol. 4, p.147, 1964.

[4] J. W. Heanton and A. C. Rose-Innes, "Critical currents of a superconductor of the second kind," *Cryogenics*, vol. 4, issue 2, pp. 85-89, 1964.

[5] Yu. F. Bychkov, V. G. Vereshchagin, M. T. Zuev, V. R. Karasik, G. B. Kurganov and V. A. Mal'tsev, "Similarity of longitudinal and transverse critical current in superconducting alloys with rigidly pinned vortex lattice," *JETP Lett.*, vol. 9 no. 12, pp. 404-407, Jun. 1969.

[6] V. R. Karasik and V. G. Vereshchagin, "Investigation of longitudinal critical currents in superconducting alloys based on Ti and Zr," *Sov. Phys. JETP,* vol. 32, no. 1, pp. 20-26, 1971.

[7] C. J. Bergeron, "Simple model for longitudinal force‐free current flow in superconductors of the second kind," *Appl. Phys. Lett.,* vol. 3, p. 63, Aug. 1963.

[8] D. G. Walmsley, "Force free magnetic fields in a type II superconducting cylinder," *J. Phys. F*, vol. 2, no. 3, p. 510, 1972.

[9] A. M. Campbell and J. E. Evetts, "Flux vortices and transport currents in type II superconductors," *Adv. Phys.*, vol. 21, issue 90, pp. 199-428, 1972.

[10] T. Matsushita, M. Kiuchi and E. S. Otabe, "Innovative superconducting force-free cable concept," *Supercond. Sci. Technol.*, vol.25, p. 125009 2012.

[11] T. Matsushita, V. S. Vyatkin, M. Kiuchi and E. S. Otabe, *TEION KOGAKU (J. Cryo. Super. Soc. Jpn.)* [in Japanese], vol. 48, p. 569 2013.

[12] B. Maiorov, Q. X. Jia, H. Zhou, H. Wang, Y. Li, A. Kursunovic, J. L. MacManus-Driscoll, T. J. Haugan, P. N. Barnes, S. R. Foltyn and L. Civale, "Effects of the Variable Lorentz Force on the Critical Current in Anisotropic Superconducting Thin Films," *IEEE Trans. Appl. Supercond.*, vol. 17, issue 2, p. 3697, 2007.

[13] A. Ibi, H. Iwai, K. Takahashi, T. Muroga, S. Miyata, T. Watanabe, Y. Yamada and Y. Shiohara, "Investigations of thick YBCO coated conductor with high critical current using IBAD-PLD method," *Physica C*, vol. 426-431 part 2, pp. 910-914, 2005.

[14] T. Kato, R. Yoshida, N. Chikumoto, S. Lee, K. Tanabe, T. Izumi, T. Haruyama and Y. Shiohara, "Microstructural characterization of GdBa₂Cu₃Oᵧ superconductive layer fabricated by in-plume pulsed laser deposition," *Physica C*, vol. 471, pp. 1012-1016, 2011.

[15] P. N. Zaitsev, G. Ockenfuss and R. Wördenweber, *Appl. Supercond.* (Inst. Phys. Conf. Ser.), vol. 158, p. 25, 1997.

[16] S. R. Foltyn, Q. X. Jia, P. N. Arendt, L. Kinder, Y. Fan and J. F. Smith, "Relationship between film thickness and the critical current of YBa₂Cu₃O₇₋δ-coated conductors," *Appl. Phys. Lett.*, vol. 75, issue 23, p. 3692, 1999.

[17] S. R. Foltyn, H. Wang, L. Civale, Q. X. Jia, P. N. Arendt, B. Maiorov, Y. Li, M.P. Maley, J. L. MacManus-Driscoll, "Overcoming the barrier to 1000 A cm width superconducting coatings," *Appl. Phys. Lett.*, vol. 87, p. 162505, 2005.

[18] S. R. Foltyn, L. Civale, J. L. MacManus-Driscoll, Q. X. Jia, B. Maiorov, H. Wang and M. P. Maley, "Materials science challenges for high-temperature superconducting wire," *Nature Materials*, vol. 6, pp. 631-642, 2007.

[19] T. Matsushita, M. Kiuchi, K. Kimura, S. Miyata, A. Ibi, T. Muroga, Y. Yamada and Y. Shiohara, "Dependence of critical current properties on the thickness of the superconducting layer in YBCO coated tapes," *Supercond. Sci. Technol.*, vol. 18, p. S227, 2005.

[20] K. Kimura, M. Kiuchi, E. S. Otabe, T. Matsushita, S. Miyata, A. Ibi, T. Muroga, Y. Yamada and Y. Shiohara, "Film thickness dependence of critical current characteristics of YBCO-coated conductors," *Physica C*, vol. 445-448, pp. 141-145, 2006.

[21] V. S. Vyatkin, K. Tanabe, J. Wada, M. Kiuchi, E. S. Otabe and T. Matsushita, "Calculation of critical current in DC HTS cable using longitudinal magnetic field effect," *Physica C*, vol. 494, pp. 135-139, 2013.

[22] T. Matsushita, V. S. Vyatkin, M. Kiuchi and E. S. Otabe, "Design of high current superconducting DC power cable using the longitudinal magnetic field configuration," *Adv. Cryo. Eng. (American Inst. Phys. Proc.)*, Vol. 1574, p. 225, 2014.

[23] V.S. Vyatkin, M. Kiuchi, E.S. Otabe, M. Ohya and T. Matsushita, "Current-carrying capacity of single layer cable using superconducting Bi-2223 tapes in a parallel magnetic field", *Supercond. Sci. Technol.*, vol. 28, 015011 (3pp), 2015.

[24] Unpublished data.

[25] E. H. Brandt, J. R. Clem and D. G. Walmsley, "Flux-Line Cutting in Type II Superconductors," *J. Low Temp. Phys.*, vol. 37, pp. 43-55, 1979.

[26] J. R. Clem and S. Yeh, "Flux-Line-Cutting Threshold in Type II Superconductors," *J. Low Temp. Phys.*, vol. 39, pp. 173-189, 1980.

[27] P. Wagenleithner, "Cutting of Bent Vortex Lines," *J. Low Temp. Phys.*, vol. 48, pp. 25-37, 1982.

[28] M. G. Blamire and J. E. Evetts, "Critical cutting force between flux vortices in a type-II superconductor," *Phys. Rev. B*, vol. 33, p.5131(R), 1986.

[29] A. Kikitsu, Y. Hasegawa and T. Matsushita, "Critical Current Density of Superconducting Nb-Ta in the Longitudinal Magnetic Field," *Jpn. J. Appl. Phys.*, vol. 25, pp. 32-36, 1986.

[30] F. Irie, T. Matsushita, S. Otabe, T. Matsuno and K. Yamafuji, "Critical current density of superconducting NbTa tapes in a longitudinal magnetic field," *Cryogenics*, vol. 29, pp. 317-320, 1989.

[31] T. Matsushita, Y. Miyamoto, A. Kikitsu and K. Yamafuji, "Critical Current Density of Superconducting Pb–Bi Alloys with Normal Bi Precipitates in a Longitudinal Magnetic Field," *Jpn. J. Appl. Phys.*, vol. 25, pp. L725-L727, 1986.

[32] T. Matsushita, "On an Enhancement of a Critical Current of Superconductors in s Longitudinal Magnetic Field," *J. Phys. Soc. Jpn.*, vol. 54, pp. 1054-1059, 1985.

[33] T. Matsushita, "Longitudinal Magnetic Field Effect in Superconductors," *Jpn. J. Appl. Phys.*, vol. 51, p. 010111, 2012.